Tomography as a Diagnostic Tool for Plasma Turbulence

A Fujisawa[1,2], Y Nagashima[1,2], K. Yamasaki[1], S Inagaki[1,2],
T Onchi[1], S Ohshima[3] and A Shimizu[4]

[1] *Research Institute for Applied Mechanics and* [2]*Research Center for Plasma Turbulence,Kyushu University, 6-1 Kasuga Kohen Kasuga, 816-8580 Japan*

[3]*Institute of Advanced Energy, Kyoto University, Kyoto University Gokasyo, Uji, Kyoto, 611-0011, Japan*

[4] *National Institute for Fusion Science, 322-6 Oroshi-cho Toki 509-5292 Japan*

Plasma turbulence consists of micro-scale fluctuations, meso-scale structures, such as zonal flows and streamers and macroscale fluctuations generated from the background micro-scale fluctuations. The modern view shows that these elemental fluctuations should interact nonlinearly with each other to produce the structure and dynamics of the turbulent plasma[**?**]. For further understanding a superior experimental method is required to observe the entire plasma turbulence with fine resolution to identify the fluctuations from micro- to macroscale. One of the diagnostics to satisfy such requirement is Computed Tomography, which can measure the entire region of plasma, probably in a sufficiently wide range of spatio-temporal scales. A prototype system has been made and installed on a linear cylindrical plasma, and has obtained the first results. This paper describes the development of the diagnostics system with the results successfully obtained with this system, and demonstrates the excellency of tomography as a diagnostic tool for plasma turbulence.

Tomography System: A trial has been performed for argon plasma discharges produced in a cylindrical device named Plasma Assembly for Nonlinear Turbulence Analysis (PANTA) [**?**]. Figure 1 shows a schematic view of the prototype system of the computed tomography. Four sets of light-guide arrays are installed on the four azimuthal directions at 45 degree apart to each other, surrounding the plasma with diameter of ∼10 cm. Each light guide array contains 33 fiber channels, and consists of collimators, optical filters, and

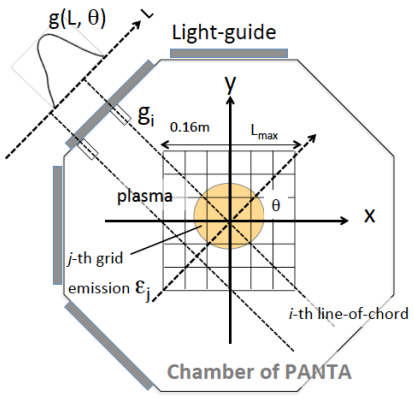

Figure 1: *A schematic view of the computed tomography system and configuration in a cylindirical plasma device named PANTA*

optical feedthrough that transfers the optically filtered light to the atmosphere side. Note that the used optical filters for ArI and ArII have their central wavelengths of 810 nm and 476.5 nm, respectively, with both full width half maximum of 30 nm. The collimators (or fiber channels) are aligned by every 5 mm in the range from $L = -8$ to $L = 8$ cm. The plasma light is passed through optical fibers to the photodiode detectors that convert the optical signals to voltage ones.

Results of Tomography: Figure 2 shows examples of the obtained results of reconstructed local emission and the temporal evolutions for ArI and ArII for a discharge with filling gas pressure of 2.5 mT, with temporally averaged emission profiles of them from 0.2 s to 0.5 s. In the process to deduce local emission, the set of the line-integrated data can be reconstructed into the local image, using Maximum Likelihood-Expectation Maximization (MLEM)[**?**]. The method, MLEM, is developed in medical application, and is chosen to be used for the tomographic reconstruction of plasma as an algorithm without any a priori assumption. Spatial discontinuity can be often expected to exist in plasma, therefore, function series expansion methods like Fourier-Bessel and Cormack's functions [**?**, **?**] are not so appropriate for the plasma tomography.

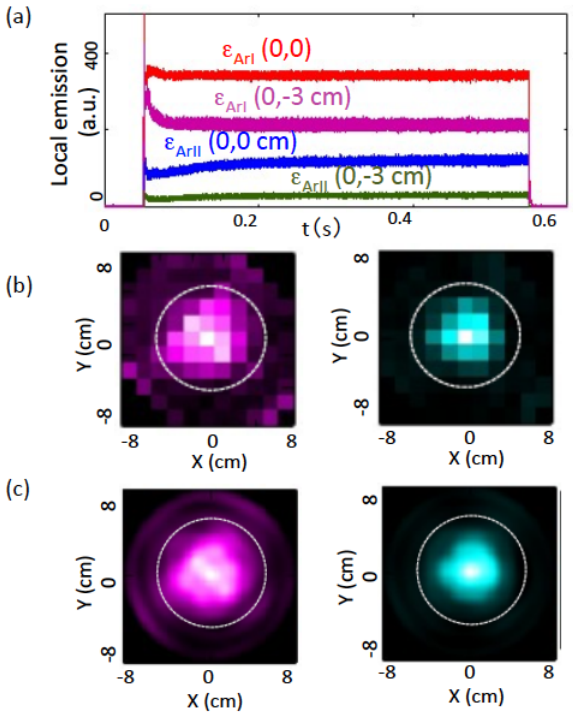

Figure 2: (a) The temporal evolutions of local emissions of ArI and ArII. (b) Temporal averaged emission profiles obtained with MLEM method for ArI and AriI. (c) The fitting image of local emission profiles with Fourier-Bessel series expansion.

The local emissions are calculated in every sampling time, here in 1 μs for the whole discharge of approximately 600 ms. The total amount of a set of tomography data is huge about 0.32 Gbyte for a shot. In order to manage the huge amount of data, the tomographic reconstruction is performed with parallel computing using totally 120 cores of 10 personal computers. As is shown in the figures, the signal levels of ArI appear larger than that of ArII. However, the signal level does not reflect the absolute ratio of their photon emissions, since in the detection system blue (or ArII) light suffers larger attenuation through the optical fiber, and lower gain

in the photodiode than infra-red (or ArI) light.

Structural Analyses: As is shown in Fig. 2(b), the emission profiles, obtained with the MLEM method, are found to be not completely symmetric around the plasma center. The asymmetry can be quantified in the decomposition into spatial Fourier components or azimuthal mode numbers, using the Fourier-Bessel Function expansion. In other words, the MLEM image can be expanded with the Fourier-Bessel function series as

$$\varepsilon(r,\theta) = \sum_n a_{0n}\hat{J}_0(k_n r) + \sum_{m,n}[a_{mn}\hat{J}_m(k_n r)\cos(m\theta) + b_{mn}\hat{J}_m(k_n r)\sin(m\theta)]$$

where $\hat{J}_m(k_n r)$ is normalized form of m-th order Bessel function. Figure 2(c) shows the results of the emission distributions after the fitting using the Fourer-Bessel series expansion.

The powers of the spatial Fourier mode components are given as the summation of the coefficients of $\hat{J}_m(k_n r)$ in Eq. (2) as $F_{FB}(m) = \sum_n (a_{mn}^2 + b_{mn}^2)$ wtih $b_{0n} = 0$. A fraction of an Fourier component is defined as $\hat{F}_{FB}(m) = F_{FB}(m)/\sum_l F_{FB}(l)$. In the case of Fig. 2(c) the fractions of the emission distributions are; $\hat{F}_{\rm FB}(0) = 97.5\%$, $\hat{F}_{\rm FB}(1) = 0.7\%$, $\hat{F}_{\rm FB}(2) = 0.6\%$, and $\hat{F}_{\rm FB}(3) = 0.7\%$ for ArI, while $\hat{F}_{\rm FB}(0) = 96.9\%$, $\hat{F}_{\rm FB}(1) = 1.9\%$, $\hat{F}_{\rm FB}(2) = 0.5\%$, and $\hat{F}_{\rm FB}(3) = 0.3\%$ for ArII. Thus, the fraction of $m = 1$ component should be dominant for the asymmetric part of ArII emission, while no spatially strong components are found for that of ArI.

Spectral Analyses: Temporal series data of plasma emissions can be decomposed to Fourier components in frequency domain. Figure 3 shows the results of Fast Fourier Transform (FFT) and wavelet spectral analyses on the data shown in Fig. 2. The FFT spectra are found to be sufficiently larger than the noise level indicated by the dashed lines. The noise levels are evaluated as the summation of the errors caused by the noises included in line-integrated signals, using the following formula,

$$\delta\varepsilon_f^2(x,y) = \sum_i \sum_j \left(\frac{\partial \varepsilon_f(x,y)}{\partial g_f(L_i,\theta_j)}\right)^2 \delta g_f^2(L_i,\theta_j), \qquad (1)$$

where $\delta g_f(L_i,\theta_j)$ and $\delta\varepsilon_f(x,y)$ mean the noise level of a line-integrated data at a frequency and the corresponding noise in the emission, respectively. The derivatives $(\partial\varepsilon/\partial g)$ can be numerically calculated.

On the other hand, the wavelet analysis shows the dynamic nature of the plasma fluctuations. The definition of the used wavelet analysis is $W_\varepsilon(f,t) = \int_{-\infty}^{\infty} \varepsilon(\tau)\Phi(f,t-\tau)d\tau$[**?**] with $\Phi(f,t) = \sqrt{f}\exp[i2\pi ft - (ft)^2/2]$, which has a natural correspondence with the traditional Fourier transformation (FFT), where the wavelet transformation has a temporal resolution of fluctuation power according to *a frequency* so as to satisfy the uncertain relation $f\delta t \sim 1$.

Discussion and Summary: A prototype of plasma turbulence tomography shows its excellent capability, demonstrating that the tomography should be able to detect plasma turbulence. One of the advantages is the non-perturbative nature. The nature extends the accessible region of the diagnostics; in the case of the PANTA plasma the traditional probes have never accessed to the inner region of $r < 2$ cm. In addition, multi-color detection can make the tomography cover the entire plasma from the outer and core region of the plasma, using ArI and ArII emission here, respectively. The tomography allows us to investigate turbulence characteristics using, the bispectral analyses to clarify the 2D nonlinear interaction between disparate scale fluctuations, the nonlinear 2D-spatial correlation of turbulence dynamics, the propagation of perturbation events in fully 2D space, and so on.

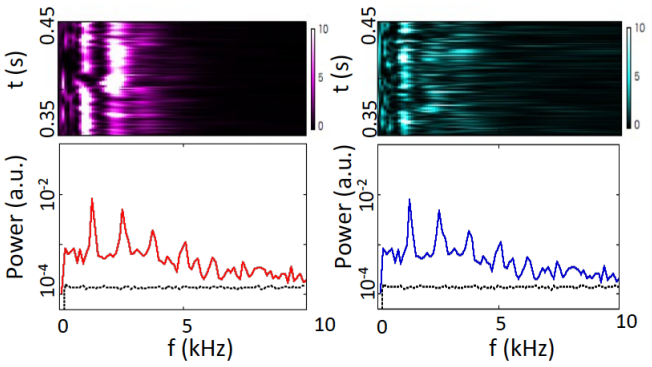

Figure 3: *Power spectra calculated with wavelet (top) and FFT (bottom). The left and right spectra show ones of ArI and ArII, respectively.*

Finally, the ultimate goal of the studies is to apply an extended system on magnetically confined plasma of high temperature. The preparation needs to develop a multi-color detection using ultra-violet and X-ray for outer and inner region of the high temperature plasma, respectively. A technique using flourescence glass has been already tested and presented successful results for UV detection[**?**]. On the other hand, the scintillation technique needs to be used for X-ray detection, although actual test should be a future work. Finally, the result demonstrates that the tomography should be used to detect local turbulence. The most challenging problem to achieve this concept is to construct the magnetically confined torus plasma specially designed for turbulence tomography.

References

[1] A. Fujisawa, Nucl. Fusion 49 (2009) 013001.

[2] S. Oldenbürger, S. Inagaki, T. KOabyashi et al., Plasma Phys. Control. Fusion **54** 055002(2012).

[3] A. Fujisawa et al., Plasma Phys. Control. Fusion 58 025005 (2016)

[4] A. Fujisawa et al., Plasma Fusion Res. **10** 1201080 (2015).

[5] L.A. Shepp and Y. Vardi, IEEE Trans. Med. Imag., **1** 113 (1982).

[6] Y. Nagayama, J. Appl. Phys. **62** 2702 (1987).

[7] A. M. Cormack, J. Appl. Phys. **35** 2908 (1964).

[8] T. Onchi, A. Fujisawa, A. Sanpei, Rev. Sci. Instrum. **85** 113502 (2014).

[9] B. Ph. van Milligen, C. Hidalgo, E. Sanchéz, Phys. Rev. Lett. **74** 395 (1995).